



Article

GIS-Based Assessment of Fire Effects on Flash Flood Hazard: The Case of the Summer 2021 Forest Fires in Greece

Niki Evelpidou ^{1,*}, Maria Tzouxanioti ¹, Evangelos Spyrou ¹, Alexandros Petropoulos ¹, Anna Karkani ¹,
Giannis Saitis ¹ and Markos Margaritis ²

¹ Faculty of Geology and Geoenvironment, National and Kapodistrian University of Athens, Panepistimiopolis, 15784 Athens, Greece

² Faculty of Civil Engineering, University of Peloponnese, 26334 Patras, Greece

* Correspondence: evelpidou@geol.uoa.gr

Abstract: Greece, like the rest of the Mediterranean countries, faces wildland fires every year. Besides their short-term socioeconomic impacts, ecological destruction, and loss of human lives, forest fires also increase the burnt areas' risk of flash flood phenomena, as the vegetation, which acted in a protective way against runoff and soil erosion, is massively removed. Among the most severe wildland fire events in Greece were those of summer 2021, which were synchronous to the very severe heat waves that hit the broader area of the Balkan Peninsula. More than 3600 km² of land was burnt and a significant amount of natural vegetation removed. Three of the burnt areas are examined in this work, namely, Attica, Northern Euboea, and the Peloponnese, in order to assess their risk of future flash flood events. The burnt areas were mapped, and their geological and geomorphological features studied. Flash flood hazard assessment was accomplished through a Boolean logic-based model applied through Geographic Information Systems (GIS) software, which allowed the prioritization of the requirement for protection by identifying which locations were most prone to flooding. The largest part of our study areas is characterized by geomorphological and geological conditions that facilitate flash flood events. According to our findings, in almost all study areas, the regions downstream of the burnt areas present high to very high flash flood hazard, due to their geomorphological and geological features (slope, drainage density, and hydrogeology). The only areas that were found to be less prone to flood events were Vilia and Varimpompi (Attica), due to their gentler slope inclinations and overall geomorphological characteristics. It is known that vegetation cover acts protectively against flash floods. However, in this case, large areas were severely burnt and vegetation is absent, resulting in the appearance of flash floods. Moreover, imminent flooding events are expected to be even more intense in the areas downstream of the burnt regions, possibly bearing even worse impacts on the local population, infrastructure, etc.

Keywords: flash floods; wildfires; natural hazard; modeling



Citation: Evelpidou, N.; Tzouxanioti, M.; Spyrou, E.; Petropoulos, A.; Karkani, A.; Saitis, G.; Margaritis, M. GIS-Based Assessment of Fire Effects on Flash Flood Hazard: The Case of the Summer 2021 Forest Fires in Greece. *GeoHazards* **2023**, *4*, 1–22. <https://doi.org/10.3390/geohazards4010001>

Academic Editors: James Hilton and Tiago Miguel Ferreira

Received: 14 October 2022

Revised: 2 December 2022

Accepted: 19 December 2022

Published: 23 December 2022



Copyright: © 2022 by the authors. Licensee MDPI, Basel, Switzerland. This article is an open access article distributed under the terms and conditions of the Creative Commons Attribution (CC BY) license (<https://creativecommons.org/licenses/by/4.0/>).

1. Introduction

Floods and especially flash floods are among the costliest natural disasters [1–7]. They usually occur after intense and/or constant rainfall events. As natural disasters, they pose a global issue, usually resulting in many fatalities, as well as infrastructure damages, crop damages, and loss of property [8]. They are a significant problem in Europe, and especially in the Mediterranean [3,9–12].

Flash floods in general are due to meteorological factors, such as rainfall intensity and duration, whereas they are facilitated or hindered by the geomorphological features of the drainage basin (e.g., drainage density, morphological slopes) and the geological conditions (e.g., rock or soil porosity), as well as land cover and management [9,13–19].

Among the most important factors that limit surface runoff and therefore the impact of flash floods is the vegetation. Plants and especially trees intercept the raindrops, and thus

less water falls on land. Not only do they absorb soil water through their roots but they also create holes in the soil, thus facilitating water infiltration. Furthermore, the presence of plants increases the soil and/or bed roughness, and hence a reduction in the water's velocity, which has more time to infiltrate. As such, surface runoff and consequentially flash flood hazard are reduced [13–15,19,20].

Forest fires are another natural disaster that affect many countries globally and whose management is considered of utmost importance. They are among the most devastating natural disasters when it comes to human activities, infrastructure, fatalities, and the environment [20]. Wildfires are a significant problem in Europe, as approximately 4500 km² of land is burnt every year [21]. The Mediterranean region is particularly prone to wildfires, due among other reasons to the presence of flammable vegetation (such as coniferous trees, bushes etc.) [22–26] in the dry summer period and the strong winds that prevail in the summer months [27,28]. Over the last decade, forest fires have increased in the Mediterranean region, due in part to the constantly increasing temperature [29].

Forest fires lead to the removal destruction of vegetation, thus causing decreases in infiltration, porosity, and organic matter [30–32] that can lead to a sudden change in the burnt area's relief and hydrological regime, [33], thus resulting in an increase in surface runoff and a decrease in infiltration [34–38]. Additionally, the heat leads to the formation of a superficial hydrophobic soil layer that further hinders water infiltration, thus increasing the runoff, as well as facilitating soil erosion [39]. It can therefore be concluded that after a wildfire, surface runoff, as well as related natural hazards, including debris flows, flash floods and surface runoff erosion, increase [32,40–42]. Many studies have been conducted that have certified this fact. Jordan et al. [43], for instance, showed that in British Columbia, after wildfires, natural hazards including landslides, debris flows and floods increased. Areu-Sangel et al. [44] proved that in Stromboli, after wildfires caused by volcanic eruptions, the flash flood hazard increased. Diakakis [45] showed that in Marathon, the flood hazard increased after the 2009 wildfires. Evelpidou et al. [46] showed that the areas affected by 2021 summer wildfires in Greece are more susceptible to surface runoff erosion. In addition, Karkani et al. [47] showed that the wildfire events before the August 9, 2020 flash flood episode in Psachna and Politika in central Euboea Island increased flash flood susceptibility. In fact, it is estimated that destruction of 10% of the forests of a region can lead to a 4% to 28% increase in flash flood frequency [48]. A very common means of massive vegetation removal are forest fires.

In Greece, forest fires occur every year. Among the most severe wildland fire events in Greece were those of 2007 and 2018. The 2021 conflagrations were among the most intense to take place in Greece as well, because the total burnt area reached roughly 3600 km² and the fires lasted for 20 days in July and August [49]. Most of the burnt areas face flash flood problems on a regular basis. Therefore, the hazard immediately after conflagrations is arguably even higher.

The purpose of this paper is to assess the effects of fire on flash flood hazard. Such a decision-support tool will provide the power to select which areas should be prioritized for flood control or surface runoff delay projects. In cases where the disaster is as devastating as it was in the summer of 2021, it is impossible to undertake projects to protect all the areas around the burnt land. It is important to have a tool that enables the prioritization of the need for protection by defining which areas are most vulnerable to inundation. In this paper, we studied the areas that burnt to the greatest extent after the 2021 wildfires, namely, Attica, Northern Euboea, and the Peloponnese, and estimated their risk of future flash flood events. The burnt areas were mapped, their geological and geomorphological features studied and mapped, and final flood hazard maps were produced using GIS software.

2. Study Areas

The three regions studied in this research were Attica, Northern Euboea, and the Peloponnese in Greece (Figure 1). The Attica regional unit (formerly prefecture) is in the Central Greece administrative region and covers an area of 3023 km². Euboea, with

an area of 3658 km², is the second-largest island of Greece (after Crete) and one of the regional units of Greece, also belonging to Central Greece. The Peloponnese is one of the geographic departments of the country and covers an area of 21,650 km². The climate is Mediterranean and characterized by mild winters and dry and hot summers. Rainfalls are not very frequent and mainly occur in the wet season (autumn and winter), yet it is not uncommon for extreme weather events to occur, such as rapid and intense rainfalls and thunderstorms. For example, the flash flood event of 9 August 2020 in Euboea Island [47] was a result of extremely heavy rainfall (297 mm) in a short period of time (8 h).

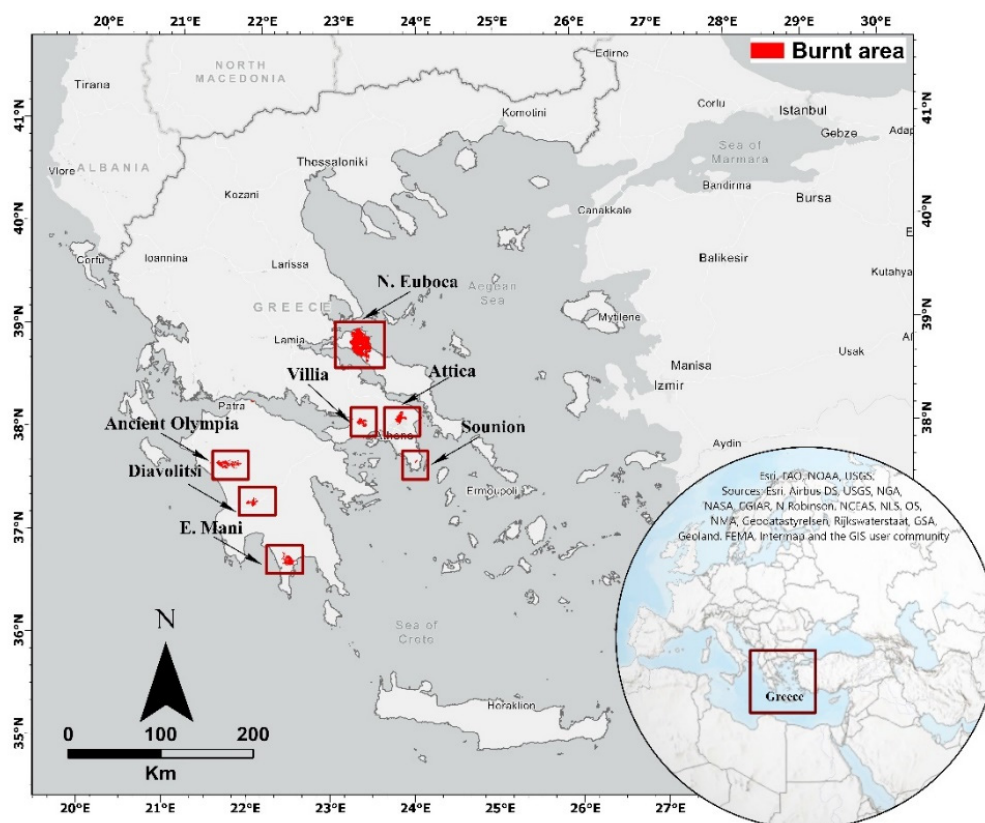


Figure 1. Location of the studied sites.

It is worth mentioning that during the summer of 2021, several heat waves struck Greece and other Mediterranean countries, with temperatures reaching and even exceeding 40 °C. The hot air facilitated the preservation and spreading of the conflagrations. Of course, no precipitation took place, and the wind intensity and direction were in many cases favorable for the spreading of the fires. In that sense, the extent and severity of the fires was inevitable [49].

2.1. Attica

In Attica Prefecture, the August 2021 wildfires affected three areas: Varimpompi, Villia, and Sounion National Forest. The burnt part in Varimpompi reached 85 km² [46,49]. Settlements within the burnt areas include Varimpompi, Ippokrateios Politeia, Tatoi, Afidnes, Pefkofyton, Aghios Stefanos, and Kryonerion (Figure 2). The urban fabric in the area, especially in the settlements of Ippokrateios Politeia, Tatoi and Afidnes, is relatively well developed. The area of Varimpompi (Figure 3) is mainly covered by Neogene sedimentary formations, primarily of lacustrine, fluvial and terrestrial origin. Limestone and dolomite are also present, whereas other lithologies such as scree, flysch, schist, and marble are rare [49]. The burnt part mainly consisted of the aforementioned sedimentary units and to a lesser extent marble and limestone/dolomite [49]. Carbonate rocks generally decrease the superficial runoff, due to the increase they cause in water infiltration through their porosity.

Other sedimentary rocks either facilitate or prevent runoff erosion, and consequently decrease or increase flash flood hazard, respectively, depending on their porosity. When it comes to land cover, the biggest part of the burnt land was covered by forest vegetation (mainly broad-leaved, coniferous and mixed forests) and transitional zones between forest and shrub vegetation, whereas a smaller part was covered by cultivable and/or cultivated areas and urban fabric, according to Corine Land Cover [50].

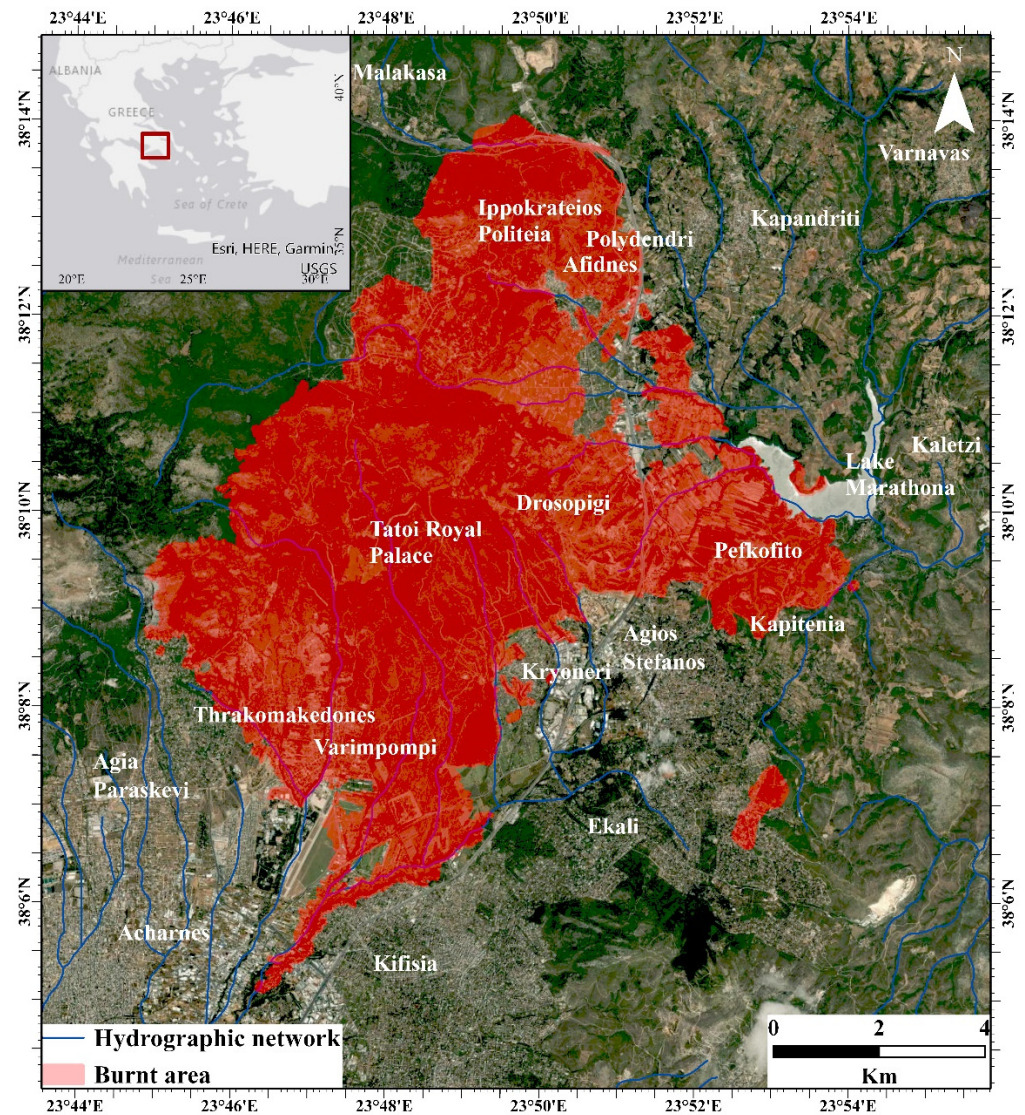


Figure 2. Areas affected in the wider area of Athens. The map is also available in web map view through the URL <https://arcg.is/1bqz1i> (accessed on 15 May 2022).



Figure 3. Part of the burnt area at Varimpompi on 6 November 2022. The exact location of Varimpompi in the wider area of Attica is shown on the map of Figure 2.

The area of Villia is almost exclusively composed of limestone, occasionally dolomite, whereas scree, alluvial and marl–clay–sandstone are also present [49]. The burnt part, reaching 66 km² [49], contains limestone and only to a very small extent scree [51]. This means that the geological structure generally decreases the surface runoff. As far as Villia is concerned, almost all of the burnt lands were covered by natural vegetation, i.e., forests, mainly sclerophyllous and coniferous, as well as shrubs and grasslands.

In Sounion National Forest, schist, and to a lesser extent marble, dominates the area [49]. The same geological regime is for the burnt part as well. Marble facilitates infiltration and decreases the flash flood hazard, contrary to schist. The total burnt area reached 55 km². As its name states, its largest part is covered by forests of several types (e.g., sclerophyllous, coniferous) and shrubs, and there was also a cultivated area. More specifically, five main vegetation units are found, each covering an almost equal area to the others. The said units include cultivations, coniferous forests, sclerophyllous forests, mixed forests and shrubs.

Based on the aforementioned, land cover facilitated the spreading of the forest fires, in association with the heat waves that had previously affected Greece. All three areas are characterized by a well-developed drainage network, which partly runs through urban areas. In the case of Varimpompi, the two rivers that dominate include Kifissos and Oinois. In Villia, the main stream has an E–W direction, although there are smaller catchments as well. When it comes to the fire-affected areas of Attica Prefecture, well-developed drainage systems partly drain urban areas. There are two main hydrographic systems in the wider area of Varimpompi. The main drainage networks are the Oinoi river, flowing towards Marathon, and the Kifissos river, flowing towards the western suburbs of Attica. In the fire-affected area in Villia, a drainage system crosses about 10 km in an E–W direction and finally ends up in the area of Elefsina [46]. There are also smaller catchments passing through the fire-affected area, flowing towards Nea Peramos. Therefore, flash flooding events are facilitated.

2.2. Northern Euboea

Regarding Euboea, the north part of the island was severely affected by the 2021 fires (Figures 4 and 5), with the burnt land reaching an area of 505 km² [46,49]. Northern Euboea is comprised of Neogene lacustrine, terrestrial and fluvio-lacustrine sediment and to a small extent ultramafic rock, carbonate and mica schist [49]. In the case of northern Euboea, according to Corine Land Cover 2018 [51], almost all of it was covered by coniferous and broad-leaved forests, whereas only a small part included cultivable land, meaning that any

fire on a small scale could easily obtain the severity of the August 2021 fires. Among the most significant settlements within the conflagrated area are Agia Anna, Rovies, Limni, Pappades, Kerasia, Vasilika and Pefki (Figure 5). The rural fabric is not well developed, as most of the area is woodland and all of the aforementioned settlements are small villages.



Figure 4. Part of the fire-affected area in northern Euboea on 3 September 2022.

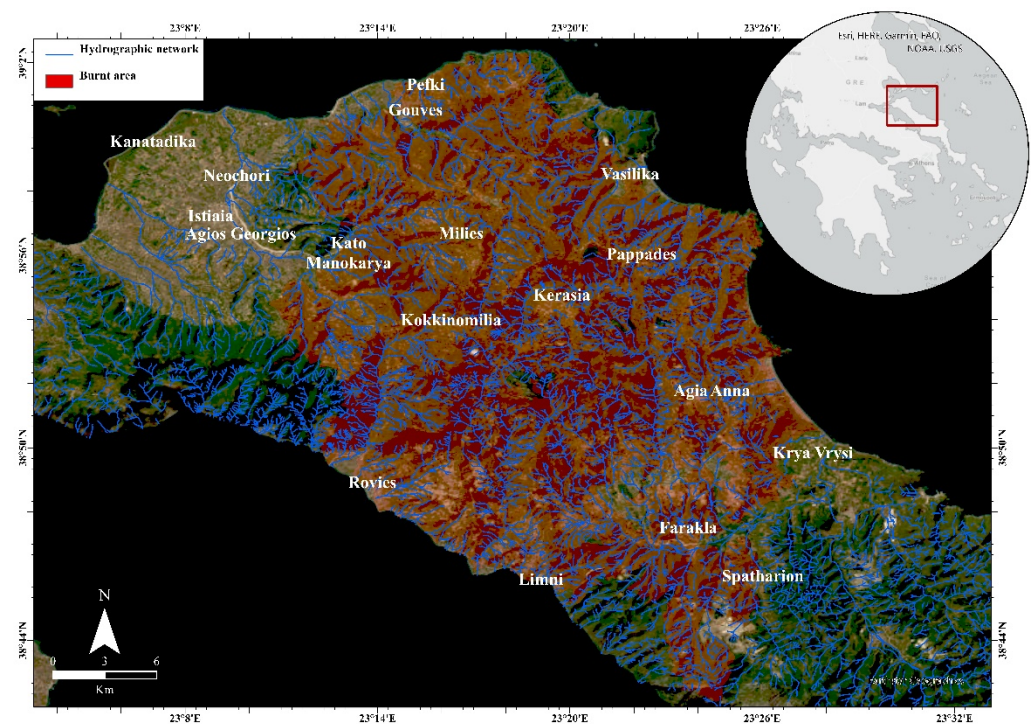


Figure 5. Areas affected in the wider area of northern Euboea Island. The map is available in web map view through the URL <https://arcg.is/1CGbqz> (accessed on 15 May 2022).

The wider area generally includes many small mountainous drainage basins with short streams, even though there are a few larger catchments. In general, the drainage networks are well developed. Most of the drainage basins are small with short hydrographic networks, yet there are a few large drainage basins covering a significant part of the fire-affected area, ending up at Gouves, Rovies, Neochori and Kria Vrysi (Figure 5).

2.3. The Peloponnese

Among the areas burnt during the summer 2021 wildfires in the Peloponnese were Ancient Olympia, Diavolitsi and East Mani. The burnt part of all areas reached a total surface area of 290 km² [46,49]. In Ancient Olympia, various clastic sedimentary rocks prevail [49]. A total of 135 km² [46,49] were burnt. Land cover mainly includes cultivations and only to a small extent forests. The affected settlements included Lampeti, Lalas and Ancient Olympia (Figure 6). The Diavolitsi burnt area had a surface of 47 km² [46,49]. It is almost entirely composed of clastic sediment (marl, sandstone, conglomerates, etc.) [49]. This area too was occupied by forests and cultivations, with the former covering a larger part than the latter. In all cases, the settlements are small villages with no significant urban fabric, mainly rural. In East Mani, the burnt area was 105 km² [46]. It is mainly covered by radiolarite, as well as a few carbonates [49]. The slopes of these burnt areas are generally high. In Olympia, for instance, half the area has a slope gradient of 10–30° and 30% exceeds 30°. In Diavolitsi, the proportion is about 60% and 25%, respectively, and in East Mani 35% and 50%, respectively. As far as the drainage basin is concerned, Ancient Olympia and East Mani host well-developed drainage basins, which is not the case for Diavolitsi. Finally, the land cover in these four areas favored the spreading of the devastating fires, even though forests covered a smaller part in comparison to the other regions (Euboea and Attica), as a significant part of them was covered by low vegetation (e.g., cultivations).

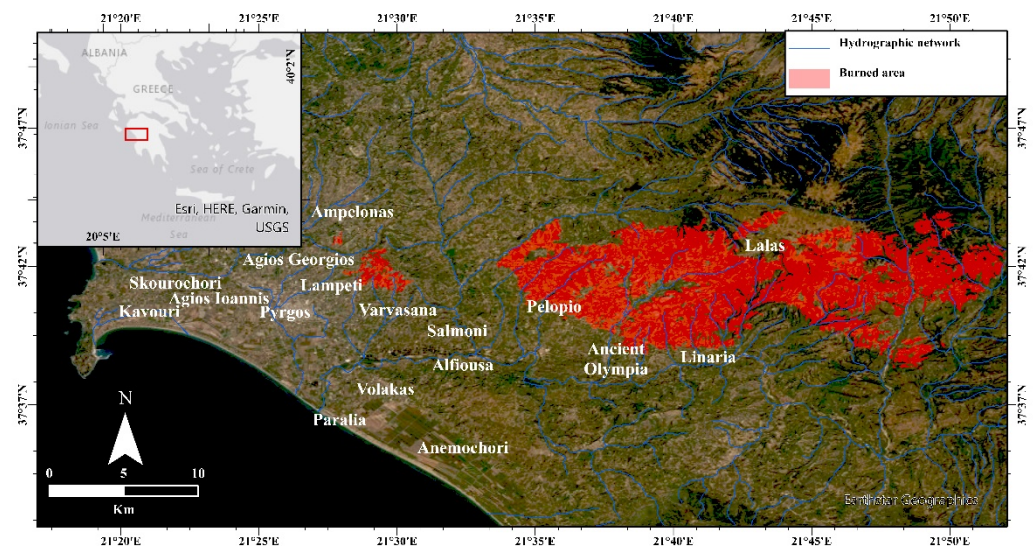


Figure 6. Areas affected in the wider area of Ancient Olympia. The map is available in web map view through the URL <https://arcg.is/TW5jy0> (accessed on 15 May 2022).

3. Materials and Methods

For the purposes of this work, the geological and geomorphological characteristics of the burnt and wider areas were studied. Data were derived from the bibliography, several measurements with GIS software (ArcGIS Pro and MapInfo Pro), and fieldwork conducted during previous research in the study areas. All collected data were imported into GIS software (ArcGIS Pro version 2.9.3 and MapInfo Pro version 12.5). Additionally, a web map has been created through the ArcGIS platform, where the burnt parts of the study areas are depicted. The web map can be accessed in this link: <https://arcg.is/1bqz1i> (accessed on 15 May 2022).

The flash flood hazard was evaluated using a Boolean logic-based model. The main parameters used were morphological slope, drainage density, hydrolithology and the burnt areas (Figure 7). Primary data used for the assessment included a high-resolution digital elevation model (DEM) of 5 × 5 m, which was derived from topographic maps at a scale of 1:5000, from the UAV survey (DJI Mavic Mini with flight elevation between 50–70 m) and RTK-GNSS (Spectra SP-80 with accuracy 0.2 m) measurements in the field. The DEM was

created in order to identify changes in the relief and in the physical characteristics of the study area.

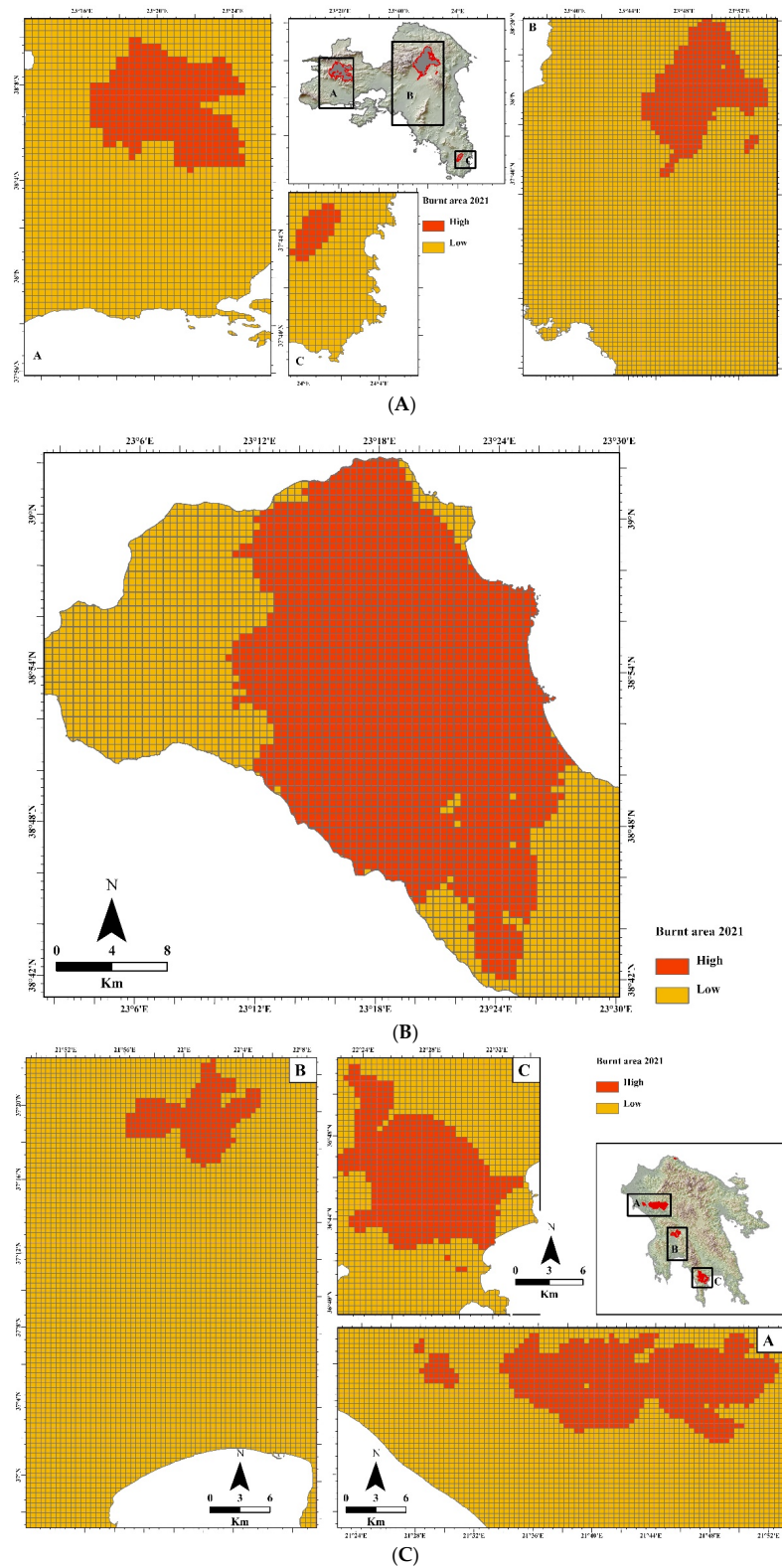


Figure 7. Fire-affected areas receiving high values in the Boolean logic rules: (A) Attica, (B) Euboea, and (C) Peloponnese.

Drainage basins were used in order to locate the upper, mid- and lower slope areas that are affected differently in an extreme flood event, as the water accumulates in low slope areas. For the flood hazard assessment, a grid of 0.5×0.5 km was created, and Boolean logic rules took place in that grid and not in the drainage basins, as their size is inhomogeneous. For example, on northern Euboea Island, the largest drainage basin has a size of 404 km². The next has a size of 152 km² and the immediate next a size of 49 km². Subsequently, 103 drainage basins with a size of 1–49 km² and more than smaller 500 drainage basins were delineated due to the existence of a well-developed hydrographic network in the study area. These rules were expressed through a set of Boolean logic rules (Table 1) and concern how the parameters will affect the downstream areas of the studied hydrological basins. According to the morphometric and physiographic features of our study areas, Boolean rules assign four values to slope parameter (high, medium, low, very low) (Figure 8), four values to drainage density (very high, high, medium, and low) (Figure 9) and three values to hydrolithology (high, medium, low) (Figure 10). The parameter given the most weight in the proposed model is the burnt area. This parameter was correlated with three other parameters, i.e., morphological slope, drainage density, and hydrolithology, in order to produce the flash flood hazard map for the downstream areas. More specifically, when the upstream area consists of a large proportion of burned fields combined with steep topography, the high value of drainage density and an impermeable bedrock, leads to inundation episodes in the low-lying downstream area. The logical rules are considered valid based on this year's flash flooding episodes in northern Euboea (Limni, Madoudi and Agia Anna), areas where the proposed model ranks the flash flood hazard of their downstream areas as high to very high. The final estimation of hazard is categorized into five values (very high, high, medium, low, and very low) based on the correlation of burnt area with the value of the other parameters (i.e., morphological slope, drainage density and hydrolithology).

Table 1. Parameters used for the assessment of flash flood hazard and their relationships. The background color follows the color plate of the map: green (low hazard), yellow (medium hazard), orange (high hazard) and red (very high hazard).

		Burned Area		
		High	Low	Medium
Parameters	Slope	Very Low–Very High	Low	Medium
	Drainage density	Very Low–Very High	Medium	High
	Hydrolithology	Low–High	High	Very High

Downstream areas in each study area are characterized by low to very low morphological slopes and low relief. As a result, parameters such as total relief or mean height do not provide valid results. Parameters such as stream power could not be calculated as no volumetric flow rate data were available. The aforementioned parameters, in combination with the parameters used in the present study, e.g., burnt area, morphological slopes, drainage density, and hydrolithology, did not produce different results. As a result, they were not taken into account.

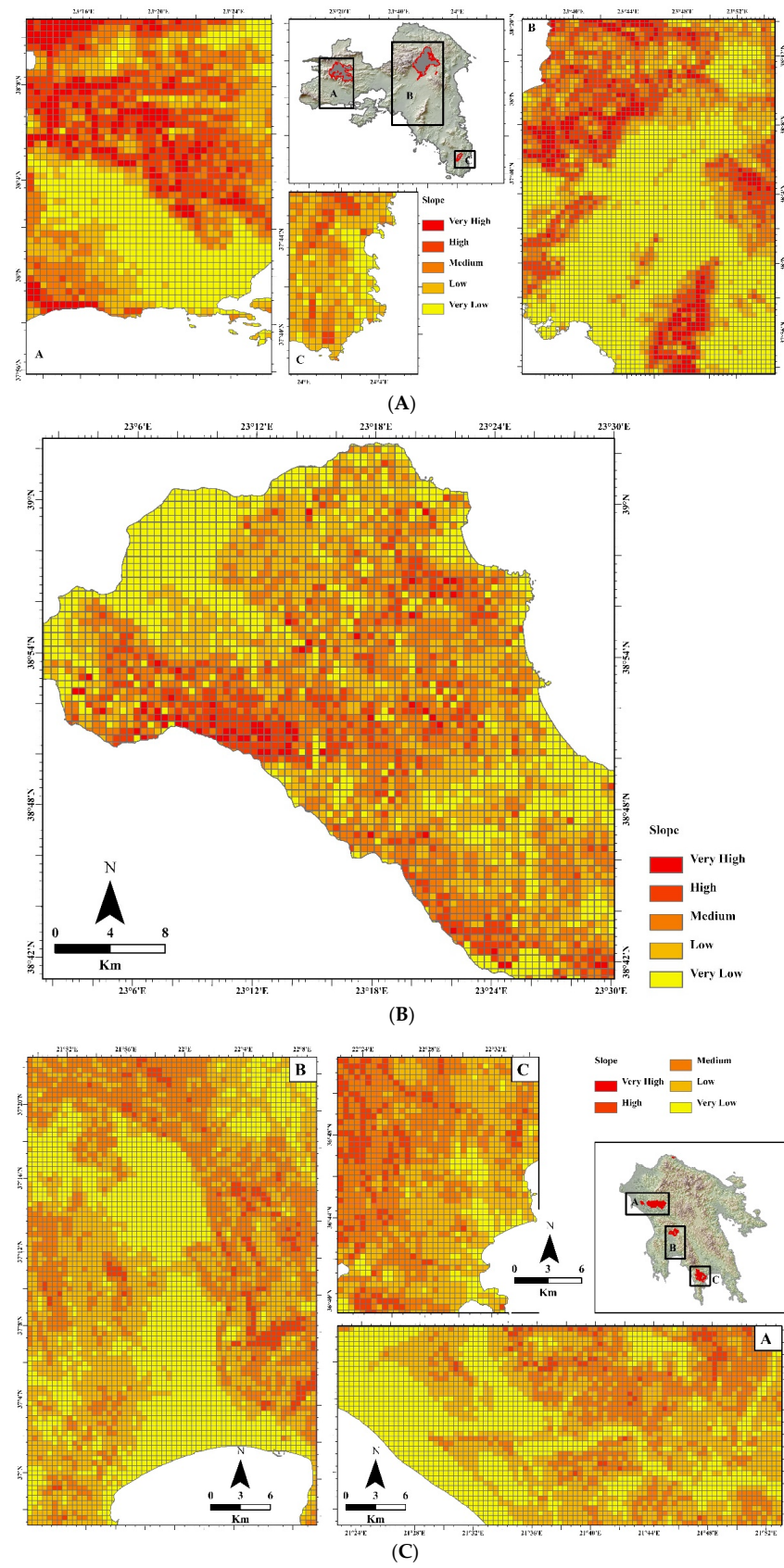


Figure 8. Classification of slope into five values: (A) Attica, (B) Euboea, and (C) Peloponnese.

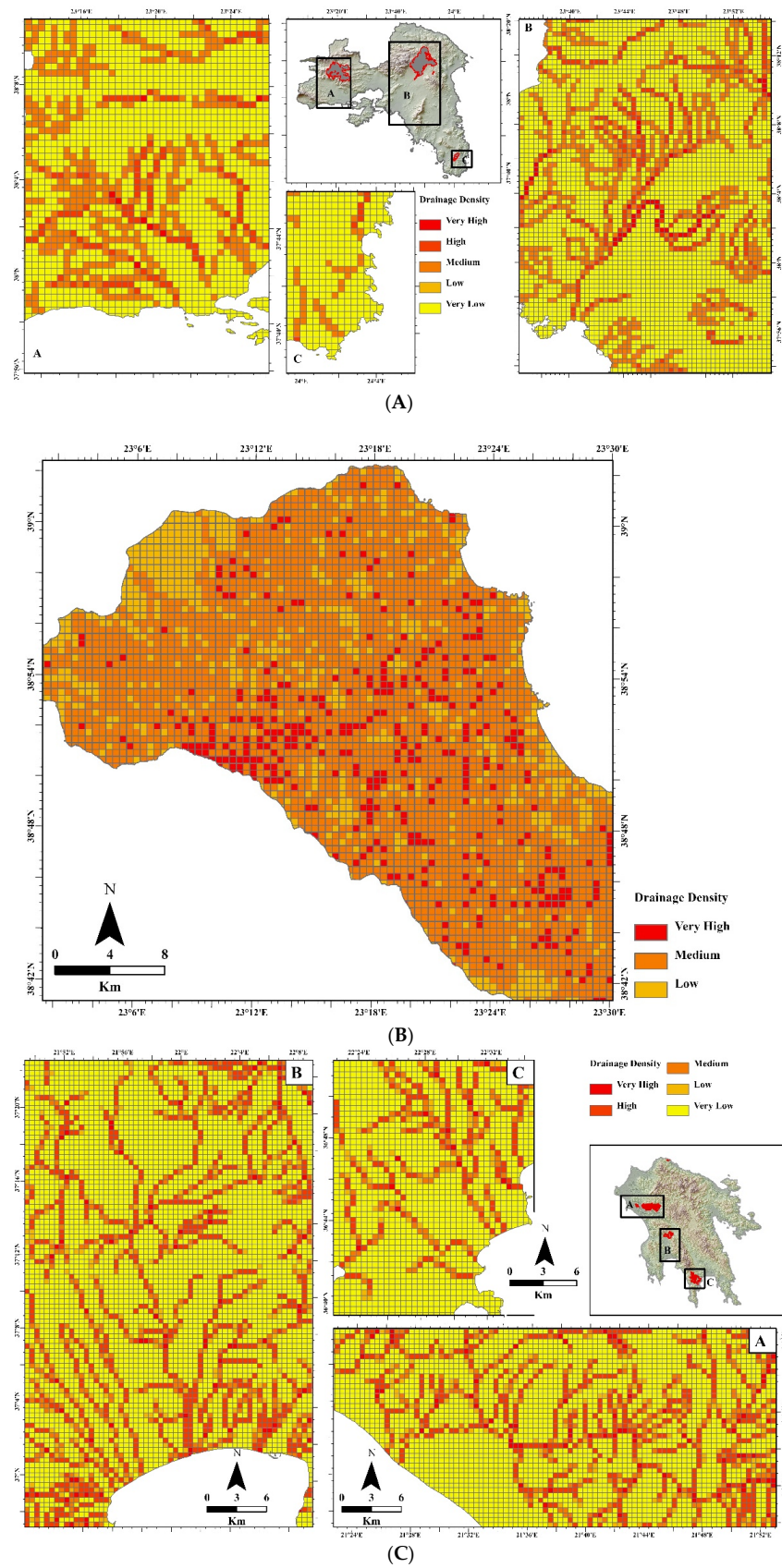


Figure 9. Classification of drainage density into three values: (A) Attica, (B) Euboea, and (C) Peloponnese.

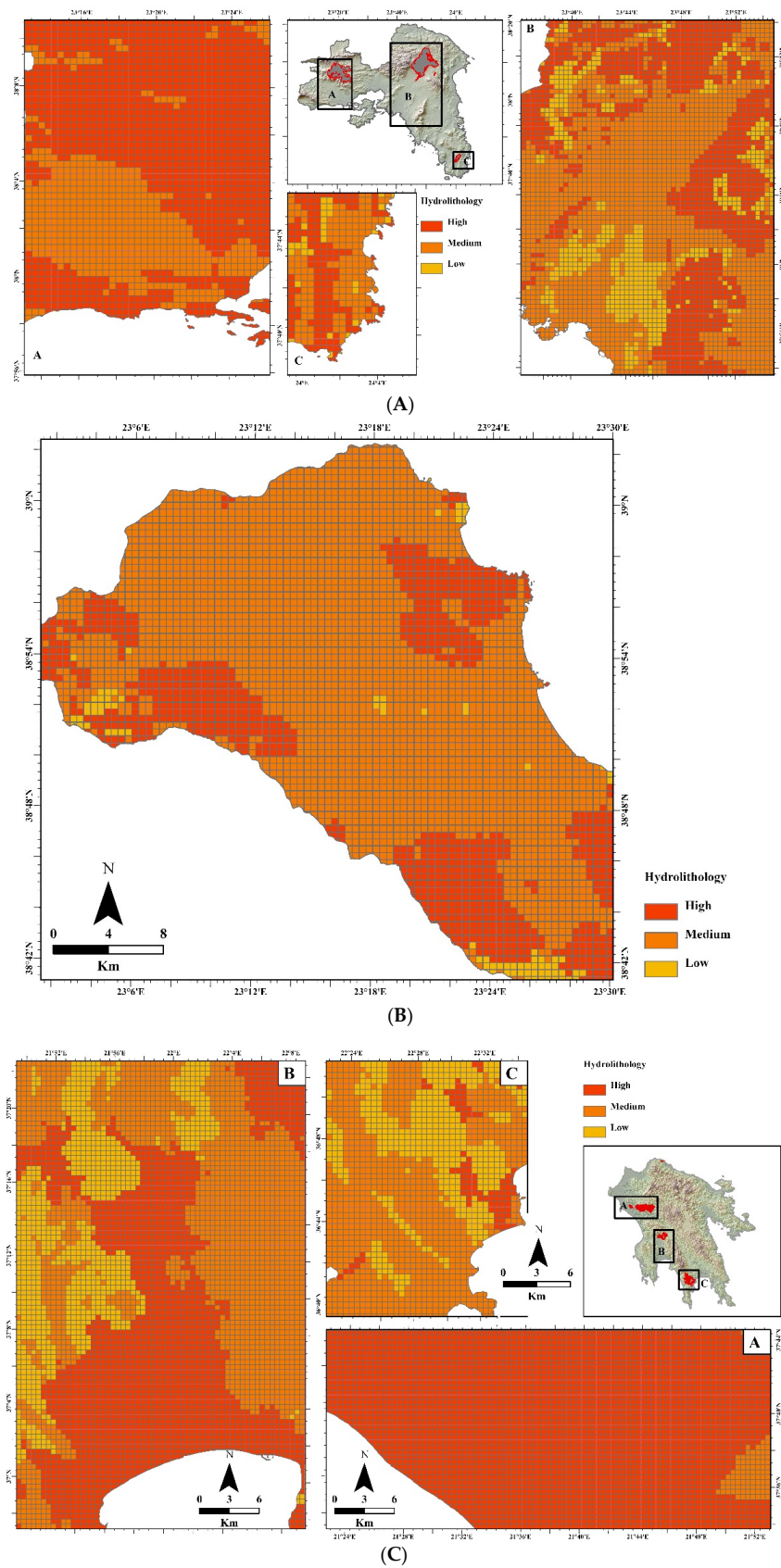


Figure 10. Classification of hydroliithology into three values: (A) Attica, (B) Euboea, and (C) Peloponnese.

4. Results and Discussion

In many countries around the world, such as Greece, there is no systematic record of hydrological parameters (e.g., discharge data). In our approach, a quantitative morphometric analysis of the drainage basin in relation to other parameters (e.g., drainage density, hydrolithology) is used for the assessment of flood hazard in large areas, such as northern Euboea Island, Attica, and the Peloponnese.

Figures 7–10 show the study areas' physiographic–morphometric characteristics (burnt areas, slope, drainage density and hydrolithology) that were used for the flash flood assessment. As far as the morphological slopes are concerned, for Attica, most parts of the burnt areas are dominated by high slopes. The morphological slope distribution of Attica is shown in Figure 8A. High gradients cover more than half of the fire-affected areas. More specifically, 53% of the area's slopes have a gradient of more than 10° , 1% of which exceeds 30° , 29% fluctuating between 4° and 10° , and 18% is characterized by a gradient of less than 4° . The fire-affected area of northern Euboea Island is characterized by abrupt slopes, downcutting erosion and dense drainage systems. More specifically, the area is characterized by high numbers of morphological slopes, small basins and short hydrographic networks. Almost 65% of the burnt area has a slope gradient of 10° to 30° and 20% more than 30° . In addition, for the wider Peloponnese area, the fire-affected areas are characterized by high elevations and steep morphological slopes (Figure 8C). In the areas of Ancient Olympia and East Mani, a well-developed drainage system is observed. In most cases, more than 80% of the burnt areas are characterized by slopes with gradients exceeding 10° . More specifically, in Ancient Olympia, slopes bearing a gradient of 10° to 30° comprise 52%, whereas those exceeding 30° comprise 28%. Only 5% is characterized by a gradient of less than 4° . Similarly, in the Diavolitsi area, 62% and 24% of the slopes have gradients of 10 – 30° and more than 30° , respectively, with flat areas (less than 4° in inclination) covering only 3% of the total area. Finally, in Mani, slopes more than 30° and 10 – 30° are almost equal, covering 48% and 35% of the burnt areas, respectively, while 11% of the area is characterized of gradients between 4 and 10° .

Figures 11–13 present the final flash flood hazard maps. Regarding the Villia region, Attica Prefecture, the flash flood hazard around the burnt area is generally characterized as low to medium, as the slope of the area is low to medium, the hydrolithology is medium, and the drainage density fluctuates between very low to high (Figure 11). High flash flood hazard is only occasionally noted north of the burnt area. This was expected, as the slope gradient in this part of the prefecture is low, even though the hydrolithology is characterized as medium to high. The drainage density is only high to the south of the burnt lands and only occasionally to the north. The narrow area around the burnt lands contains one northern drainage basin whose streams flow eastwards and a southern one whose streams flow southeastwards. When it comes to the burnt area of the northern basin, the region downstream is characterized by medium to very high flash flood hazard. The lower the altitude along the basin, the higher the flash flood hazard, the same as for the southern basin as well: the flash flood hazard is medium to high immediately downstream of the burnt region and becomes high to very high as the altitude is reduced.

As far as Varimpompi area is concerned, the region east and west of the burnt lands is characterized by low to medium flash flood hazard (Figure 11). Conversely, the lowland areas downstream, such as the alluvial plain of Kifissos, are characterized by a very high flash flood hazard, as the slope of the drainage basin downstream is very low and a large proportion of the drainage basin upstream is burnt.

In the case of Sounion National Forest (Figure 11), slope values around the burnt areas are low to medium, whereas hydrolithology is characterized as medium to high. The drainage network is characterized by very low to low drainage density, thus bearing a minimum impact on the flash flood hazard. Overall, the hazard in the area is characterized as low to medium, except for the eastern part, where it is very high, as the hydrolithology of the area is medium, the slopes downstream are very low, and upstream the drainage basin is burnt.

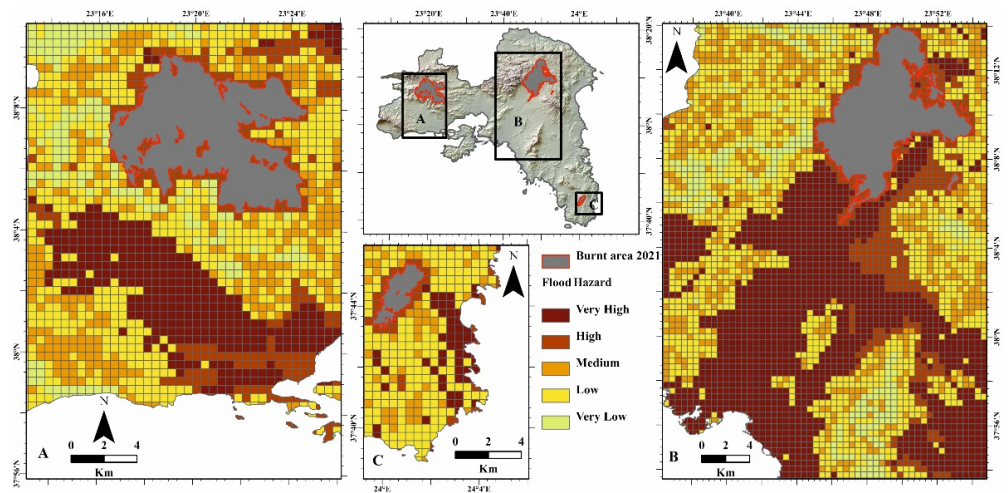


Figure 11. Flash flood hazard in the fire-affected area of Attica using a Boolean logic-based model: (A) Villia, (B) Varimpompi, and (C) Sounion National Forest.

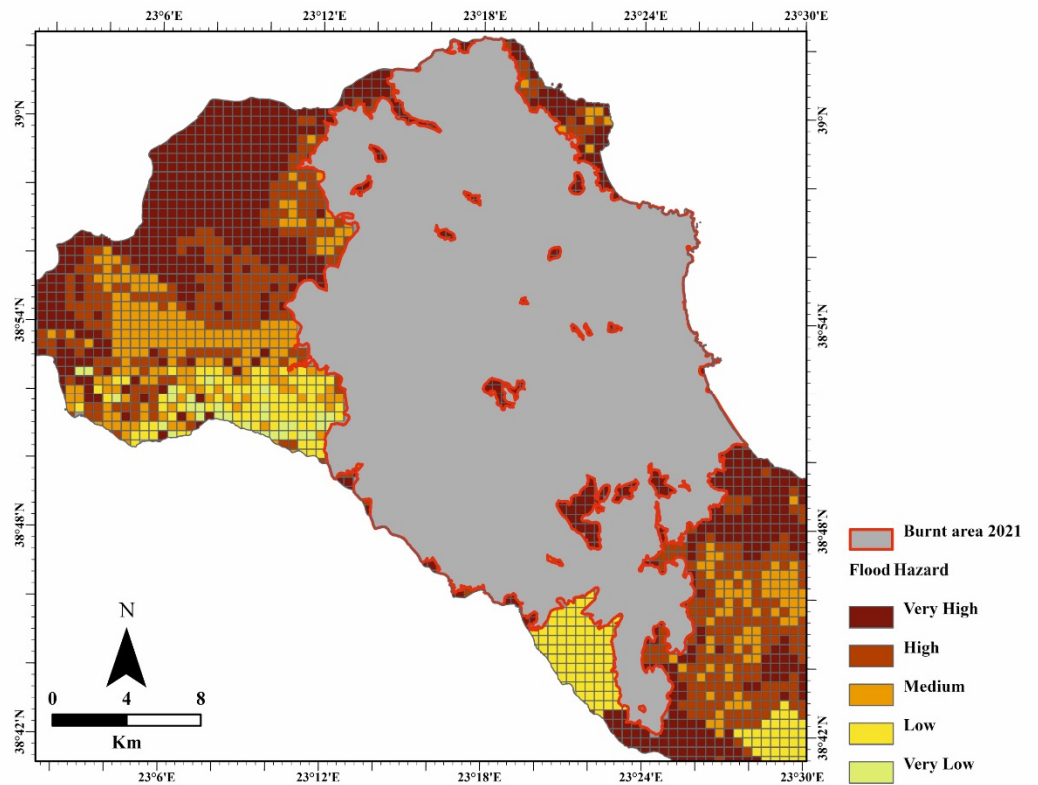


Figure 12. Flash flood hazard in the fire-affected area of northern Euboea using a Boolean logic-based model.

Northern Euboea has high to very high values regarding slopes, hydrolithology and drainage density. The flash flood hazard is characterized primarily as high to very high in almost all areas around the burnt lands (Figure 12). Low values are noted on the southeast and southwest coasts, where coastal slopes are of high values. Amongst the very high and high flash flood hazard areas are villages and smaller settlements with a fairly large population.

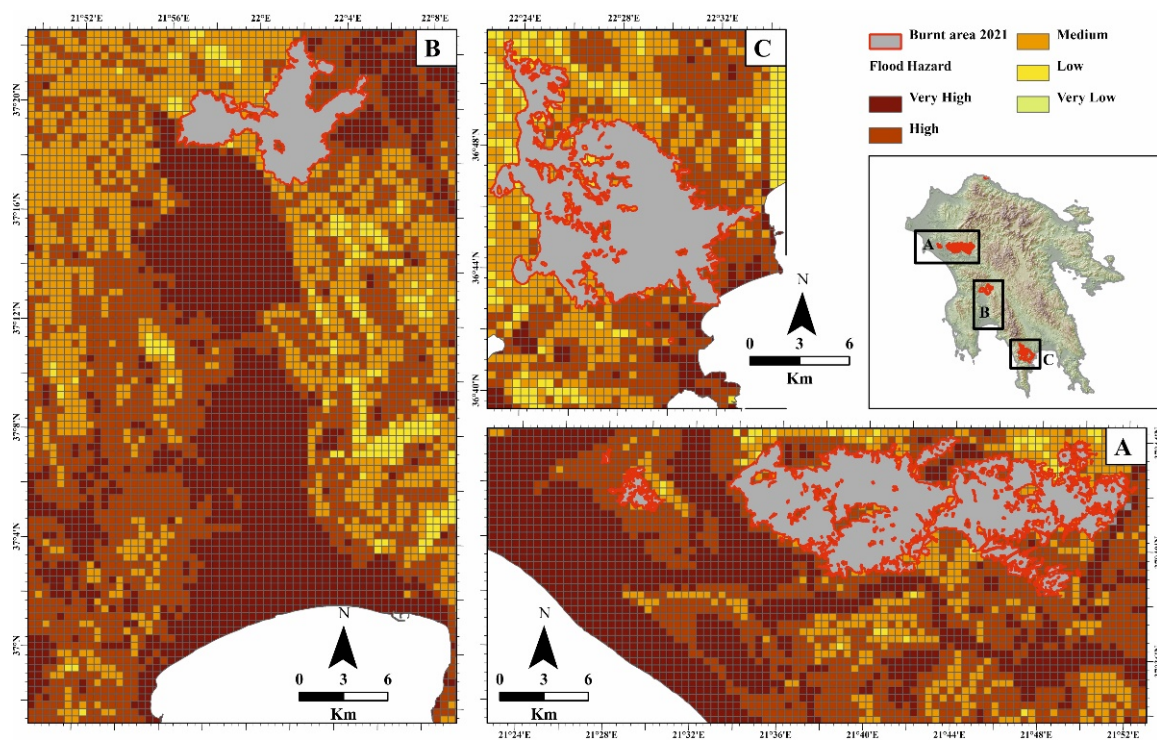


Figure 13. Flash flood hazard in the fire-affected area of Peloponnese using a Boolean logic-based model: (A) Ancient Olympia, (B) Diavolitsi, and (C) East Mani.

In the Peloponnese (Figure 13), the Ancient Olympia region is mainly characterized by very low, low and medium slopes, the drainage density being generally medium, except for the parts close to the main streams, which are of high to very high values. The main drainage basin flows southwestwards. The areas downstream of the burnt lands are mainly characterized by high and very high flash flood hazard.

In the Diavolitsi area, the slope gradient is low to very high around the burnt part. Drainage density values are generally medium, with high and very high values appearing close to the main streams. In the narrow area of the burnt part, there are two drainage basins: the eastern one flows northwards, whereas the western one flows southwards. Both are characterized by the same flash flood hazard profile: downstream of the burnt part, the hazard is high, becoming very high further downstream.

Finally, in East Mani, slope values vary from medium to very high around the burnt part, the highest values being northwest of the burnt part. Drainage density has the same values, and the highest ones appear northeast of the burnt parts. There are three main drainage basins, whose borders run NE–SW. From north to south, they flow southwards, southeastwards, and southwestwards. In all cases, flash flood hazard is high around the burnt areas (upstream), but very high immediately downstream until the coastal zone.

As has already been mentioned, burnt areas are more prone to flash flooding phenomena than unburnt ones [32,33,40,42,52]. The same flash flooding event is expected to be more severe when it takes place on a burnt area than if it took place over an area unaffected by fire [53]. It should be noted here that local administration in some of the burnt areas has already taken measures for flash flood protection, such as log erosion barriers and gabion boxes. In Attica, some measures were applied a few months after the 2021 fires around Varimpompi: log erosion barriers have been placed for the retention of rainwater and the supply of groundwater in order to keep the water in the aquifer of the area and to contribute to the faster revitalization of the ecosystem (Figure 14).



(a)



(b)

Figure 14. Examples of flash flood protection measures in Attica region (photo credit for b: A. Geramoutsos). Photos taken (a): 3 November 2021, (b): 16 December 2021.

As shown, in all our study areas (except for Varimpompi, Attica prefecture), flash flood hazard is medium to very high downstream of the burnt parts (the hazard values increasing downstream). This is due to the geomorphological and geological features of the study areas (primarily slope, drainage network and hydrolithology), which means that in these regions, even if they had not been burnt, they would still be very hazardous to inundation phenomena. The fact that parts of the drainage basins were conflagrated means that the parts downstream of the burnt lands are even more prone to future flash flooding

phenomena. Therefore, relatively intense flash flooding events were to be expected anyway, but after the intense wildfires took place, not only is the intensity and the frequency of the imminent flash flood events expected to be even higher, but the possibility of their occurrence is expected to increase as well.

The Mediterranean countries are among the European countries that face the severest issues regarding both flash floods and wildfires [22–26]. In several case studies from the Mediterranean, much research has been conducted showing that after a conflagration, flood and soil erosion hazard was increased. For instance, a high-intensity experimental fire was studied by Stoof et al. [54] in order to assess the hydrological response of a small catchment in Portugal. To achieve this, they monitored rainfall, canopy interception, streamflow, and soil moisture before and after the fire. According to their findings, an important factor was vegetation removal, which played a significant role in the increase in streamflow after the fire. Stoof et al. [54] also noted streamflow volumes increased by 1.6 times more than predicted, which resulted in increased runoff and changed rainfall–streamflow relationships; however, it is stressed that the catchment scale is important in assessing fire impact on hydrology.

Boolean logic was used in this paper. Mathematically, Boolean logic in the restricted sense, as proposed by George Boole in 1847, consists of two values, namely, 0 and 1, corresponding to “totally true” and “totally wrong”, with all intermediate values being absent. In geography-related studies, for the classification of an area, several values (usually 3 to 5) are used. For instance, for natural hazard studies, such as the present one, two Boolean values could be “high hazard” and the “medium hazard”. This means that a specific geographical unit is only characterized by high hazard and another one by medium hazard, whereas intermediate hazard values will be inexistent for all geographical units of the study area. In other words, each Boolean value can either be accepted or rejected for every geographical unit.

A major drawback of applying Boolean logic to assessing the natural disaster hazard is that for the individual geographical units, the accuracy is not always high, as the hazard values are not continuous. For example, if there exist four categorizations, namely, low, medium, high and very high hazard, each geographical unit will only have one of these four values and the intermediate ones will not be existent in the produced map (even though, of course, they will exist in reality). If two geographical units are characterized by “high hazard”, it is very possible that the actual hazard value is not the same in these two units, but slightly higher in one of them. Through the Boolean approach, however, they will be considered as having the same hazard value. The lack in accuracy from the application of the Boolean method for the assessment of flood susceptibility has been shown by Yalcin and Akyurek [55], who made an assessment of the flood hazard in the drainage basin of Bartın River (central-north Turkey) using the Boolean method (and other methods) and compared the results with historical flood series over the past 100 years.

When assessing and mapping natural disaster hazard, this method can be particularly useful for areas where the flooding phenomena are determined to a great extent by the catchment’s geological, geomorphological, physiographic, land cover and anthropogenic features, on condition that these are well known. Several authors have made flood hazard assessments and corresponding maps based on Boolean logic rules that have been applied in study areas’ physiographic, geomorphological and geological features, such as Yalcin and Akyurek [55] in Bartın River, Turkey; Mousavi and Rostamzadeh [56] in Marand Basin, Iran; and Sönmez and Bizimana [57] in Waverly, Iowa, USA.

Another method frequently used to assess an area’s risk of flood events is the analysis of the morphometric features of the area. Assessing a catchment’s susceptibility to inundation based on its morphometric characteristics can potentially lead to high-accuracy data produced, because the latter do affect flood hazard. Several authors have used this method to assess the flood hazard of various areas, such as Bhat et al. [58] in the Upper Jhelum basin, Pakistan; Lóczy et al. [59] in Tisza River, Hungary; and Farhan and Anaba [60] in Wadi Yutum, Jordan. An advantage of this method compared to the Boolean method is

that the accuracy is higher, given that the factors affecting the flood hazard are taken into account for each geographical unit. The main drawback of this method compared to the Boolean method is the difficulty in acquiring the necessary morphometric data, especially in mountainous catchments such as those prevailing in Greece and other Mediterranean countries, where hydrological and morphometric measurements are very scarce.

There are few studies that combine the morphometric characteristics of a catchment with the Boolean method in order to assess the flood hazard. The combination of these two methods has several advantages. Initially, the Boolean method based on the catchment's morphology, physiography, geology, land cover and human interventions is very easily applied in most catchments, as long as the said features are well known and mappable. Combined with the usage of the morphometric parameters, the accuracy of the produced map is significantly expected to increase.

Cosandey et al. [61] studied the post-fire and post-reforestation flood susceptibility of Southern France. They observed that of all the burnt areas in various catchments, the ones where the forest had not been burnt, and those that had been reforested showed lower peak flows than those that lacked vegetation. It is worth mentioning that in some cases, flood intensity was higher for some of the forested catchments, but water infiltration was high enough so that peak flows did not exceed those of the burnt catchments [61]. The researchers also concluded that for a specific drainage basin, covered by bedrock and with only limited soil, flood hazard was affected to a minimum extent by the forest fires, as the infiltration rates were not reduced due to the fires [61]. Moreover, they showed that surface runoff is primarily affected by the presence of vegetation itself, rather than its type (e.g., forest or grasslands).

More specifically, when it comes to our study areas, they all show an increased flash flood hazard, especially immediately after wildfires. For example, Theochari and Baltas [62] conducted a hydrological study in northern Euboea, indicating that after the 2021 wildfire, the catchments showed an increase in the peak discharges, which in fact increased as the burnt area increased. Simultaneously, the lag time between peak rainfall and peak discharge decreased in the burnt catchments [62]. It should be mentioned that this area is already prone to flash floods, not only due to its geomorphological characteristics but its high extent of urbanization as well [47]. This means that following the 2021 conflagration, which was among the severest forest fire events on the island [49], flood hazard is expected to be very high.

When it comes to the western Peloponnese, Diakakis et al. [63] conducted a study on the 2007 wildfires' impacts on the region's flood susceptibility. More specifically, they studied the inundation frequency for the pre- (1988–2007) and post-fire period (2007–2016). During the two periods, the authors identified 16 and 25 events, respectively, i.e., an average of 0.84 events per year before the conflagrations and 2.77 events per year after them [63]. Regarding mass movements, they identified 12 and 16 events (0.63 and 3.56 per year) before and after the fires, respectively [63].

Finally, as regards Attica, Alonistioti et al. [64] studied the post-fire hydrological response of several Attica catchments and found that as the burnt area increases, so does the peak discharge, their relationship being relatively linear [64]. Moreover, they observed that there was a linear relationship between the peak discharge range (before and after the wildfires) and the burnt surface. They also showed that—especially after a fire—the peak discharges were mainly affected by rainfall intensity, rather than quantity [64].

The aforementioned studies confirm that wildfires increase an area's exposure to both flash flood events and soil erosion/degradation. This is especially the case of the Mediterranean, where flood and erosion issues are already high. Based on our research in the regions of Attica, northern Euboea and the western Peloponnese, we conclude that they were already very prone to inundation events due to their geological and geomorphological characteristics, but after the severe 2021 conflagrations, their hazard is expected to increase to a very significant extent. More specifically, according to our results, the most hazardous areas in northern Euboea are Rovies, Neohori, Krya Vrysi, Vasilika, Artemisio, Istiaia,

Gouves, Madoudi, Aghia Anna, and Limni and also the smaller areas located nearby. In Athens, the most hazardous areas are Acharnes, Marousi, Ilion, Athens, Chalandri, Egaleo, Kallithea, Piraeus, Peania, Megara, Vlichada, Nea Peramos, Lakka Kalogirou, and Lavrion, and the smaller areas located nearby. Finally, the most hazardous areas in the Peloponnese are Diavolitsi, Messinia, Kalamata, Meligala, Yithion, Mavrovpuni, Vathi, Kamares, Pyrgos, Anciens Olympia, Pelopio, and Krestena and the smaller areas located nearby. Last but not least, the flood event that took place in November 2021 in the Istiaia area, an area that our method characterizes as hazardous, validate our approach.

5. Conclusions

The summer 2021 forest wildfires were among the most intense and damaging wildfires to strike Greece in decades. Therefore, the damage caused in the local low vegetation and forests was great, which means that the characteristics and the negative impacts of potential flash flood events are even greater. The quoted case studies indicate that the flood hazard, which is already high in the Mediterranean region, is increased to a very significant extent immediately or shortly after severe conflagration events. Our results confirm that the study areas, northern Euboea, the western Peloponnese and the region of Sounion, Attica, are characterized by geological and geomorphological features that facilitate flash flood events downstream of the burnt areas. This means that after the wildfires of summer 2021, due to which a very significant surface was burnt in each region and a very large vegetation cover (mainly forests) was destroyed, flood hazard is expected to be highly increased, thus creating the need for protection and mitigation measurements by the local authorities to minimize the fire impacts to the maximum possible extent. In the case of wildfires, post-fire management is difficult because of the large areas that are at risk. For this reason, it is necessary to determine high hazard areas and plan more efficiently which projects need to take place and were. Given the fact that in most cases, the high hazard areas are populated, it is necessary that measures are taken in order to prevent the loss of human lives and protect properties and infrastructures. This methodology could be used for the assessment of flood hazard in small scale areas worldwide, and it could be improved in the future by adding socioeconomic factors.

Author Contributions: Conceptualization, N.E.; methodology, N.E., M.T.; formal analysis, N.E., A.K., M.T., E.S., M.M., G.S. and A.P.; investigation, N.E., A.K., M.T., E.S., M.M., G.S. and A.P.; writing—original draft preparation, N.E., A.K. and E.S.; writing—review and editing, N.E., A.K., M.T. and E.S.; visualization, M.T.; supervision, N.E. All authors have read and agreed to the published version of the manuscript.

Funding: This research received no external funding.

Data Availability Statement: Data are available upon request.

Conflicts of Interest: The authors declare no conflict of interest.

References

1. Ahmadalipour, A.; Moradkhani, H. A data-driven analysis of flash flood hazard, fatalities, and damages over the CONUS during 1996–2017. *J. Hydrol.* **2019**, *578*, 124106. [[CrossRef](#)]
2. Jonkman, S.N. Global Perspectives on Loss of Human Life Caused by Floods. *Nat. Hazards* **2005**, *34*, 151–175. [[CrossRef](#)]
3. Barredo, J.I. Major flood disasters in Europe: 1950–2005. *Nat. Hazards* **2007**, *42*, 125–148. [[CrossRef](#)]
4. Barredo, J.I. Normalised flood losses in Europe: 1970–2006. *Nat. Hazards Earth Syst. Sci.* **2009**, *9*, 97–104. [[CrossRef](#)]
5. Flack, D.L.A.; Skinner, C.J.; Hawkness-Smith, L.; O'Donnell, G.; Thompson, R.J.; Waller, J.A.; Chen, A.S.; Moloney, J.; Largeron, C.; Xia, X.; et al. Recommendations for Improving Integration in National End-to-End Flood Forecasting Systems: An Overview of the FFIR (Flooding From Intense Rainfall) Programme. *Water* **2019**, *11*, 725. [[CrossRef](#)]
6. Hosseinzadehtalaei, P.; Tabari, H.; Willems, P. Satellite-based data driven quantification of pluvial floods over Europe under future climatic and socioeconomic changes. *Sci. Total Environ.* **2020**, *721*, 137688. [[CrossRef](#)] [[PubMed](#)]
7. Khajehei, S.; Ahmadalipour, A.; Shao, W.; Moradkhani, H. A Place-based Assessment of Flash Flood Hazard and Vulnerability in the Contiguous United States. *Sci. Rep.* **2020**, *10*, 448. [[CrossRef](#)]
8. Merz, B.; Kreibich, H.; Schwarze, R.; Thielen, A. Review article “Assessment of economic flood damage”. *Nat. Hazards Earth Syst. Sci.* **2010**, *10*, 1697–1724. [[CrossRef](#)]

9. Kundzewicz, Z.W.; Pin'skwar, I.; Brakenridge, G.R. Changes in river flood hazard in Europe: A review. *Hydrol. Res.* **2018**, *49*, 294–302. [[CrossRef](#)]
10. Kundzewicz, Z.W.; Pińskwar, I.; Brakenridge, G.R. Large floods in Europe, 1985–2009. *Hydrol. Sci. J.* **2013**, *58*, 1–7. [[CrossRef](#)]
11. Gaume, E.; Bain, V.; Bernardara, P.; Newinger, O.; Barbuc, M.; Bateman, A.; Blaškovičová, L.; Blöschl, G.; Borga, M.; Dumitrescu, A.; et al. A compilation of data on European flash floods. *J. Hydrol.* **2009**, *367*, 70–78. [[CrossRef](#)]
12. Perrin, J.L.; Tournoud, M.G. Hydrological processes controlling flow generation in a small Mediterranean catchment under karstic influence. *Hydrol. Sci. J.* **2010**, *54*, 1125–1140. [[CrossRef](#)]
13. Wilson, E.M. *Engineering Hydrology*, 4th ed.; MacMillan Press Ltd.: London, UK, 1990.
14. Smith, K.; Ward, R. *Floods: Physical Processes and Human Impacts*; John Wiley & Sons Ltd.: London, UK, 1998.
15. Ward, R.C. *Principles of Hydrology*, 4th ed.; McGraw-Hill: London, UK, 2000.
16. Bull, L.J.; Kirkby, M.J.; Shannon, J.; Hooke, J.M. The impact of rainstorms on floods in ephemeral channels in southeast Spain. *Catena* **2000**, *38*, 191–209. [[CrossRef](#)]
17. Camarasa Belmonte, A.M.; Segura Beltrán, F. Flood events in Mediterranean ephemeral streams (ramblas) in Valencia region, Spain. *Catena* **2001**, *45*, 229–249. [[CrossRef](#)]
18. Lana, X.; Martínez, M.D.; Serra, C.; Burgueño, A. Spatial and temporal variability of the daily rainfall regime in Catalonia (northeastern Spain), 1950–2000. *Int. J. Climatol. A J. R. Meteorol. Soc.* **2004**, *24*, 613–641. [[CrossRef](#)]
19. Diakakis, M. *Flood Hazard Assessment with the Use of Modeling Techniques*; National and Kapodistrian University of Athens: Athens, Greece, 2012.
20. Petropoulos, G.P.; Kontoes, C.; Keramitsoglou, I. Burnt area delineation from a uni-temporal perspective based on Landsat TM imagery classification using Support Vector Machines. *Int. J. Appl. Earth Obs. Geoinf.* **2011**, *13*, 70–80. [[CrossRef](#)]
21. Chuvieco, E.; Congalton, R. Mapping and inventory of forest fires from digital processing of TM data. *Geocarto Int.* **1988**, *3*, 41–53. [[CrossRef](#)]
22. Barbero, M.; Loisel, R.; Quézel, P.; Richardson, D.; Romane, F. Pines of the Mediterranean basin. In *Ecology and Biogeography of Pinus*; Richardson, D.M., Ed.; Cambridge University Press: Cambridge, UK, 1998; pp. 153–170.
23. Mitsopoulos, I.; Trapatsas, P.; Xanthopoulos, G. SYPYDA: A software tool for fire management in Mediterranean pine forests of Greece. *Comput. Electron. Agric.* **2016**, *121*, 195–199. [[CrossRef](#)]
24. Kozłowski, T.T.; Ahlren, C.E. *Fire and Ecosystems*; Academic Press: New York, NY, USA, 1974.
25. De la Rosa, J.M.; González-Pérez, J.A.; González-Vázquez, R.; Knicker, H.; López-Capel, E.; Manning, D.A.C.; González-Vila, F.J. Use of pyrolysis/GC–MS combined with thermal analysis to monitor C and N changes in soil organic matter from a Mediterranean fire affected forest. *Catena* **2008**, *74*, 296–303. [[CrossRef](#)]
26. Athanasakis, G.; Psomiadis, E.; Chatziantoniou, A. High-resolution Earth observation data and spatial analysis for burn severity evaluation and post-fire effects assessment in the Island of Chios, Greece. *Proc. SPIE* **2017**, *10428*, 104281.
27. Werth, P.; Potter, B.; Clements, C.; Finney, M.; Goodrick, S.; Alexander, M.; Cruz, M.; Forthofer, J.; McAllister, S. *Synthesis of Knowledge of Extreme Fire Behavior: Volume I for Fire Managers*; U.S. Department of Agriculture, Forest Service, Pacific Northwest Research Station: Portland, OR, USA, 2011.
28. Vieira, D.C.S.; Serpa, D.; Nunes, J.P.C.; Prats, S.A.; Neves, R.; Keizer, J.J. Predicting the effectiveness of different mulching techniques in reducing post-fire runoff and erosion at plot scale with the RUSLE, MMF and PESERA models. *Environ. Res.* **2018**, *165*, 365–378. [[CrossRef](#)] [[PubMed](#)]
29. Founda, D.; Giannakopoulos, C. The exceptionally hot summer of 2007 in Athens, Greece—A typical summer in the future climate? *Glob. Planet. Change* **2009**, *67*, 227–236. [[CrossRef](#)]
30. Neary, D.G.; Ryan, K.C.; DeBano, L.F. *Wildland Fire in Ecosystems: Effects of Fire on Soils and Water*; U.S. Department of Agriculture, Forest Service, Rocky Mountain Research Station: Fort Collins, CO, USA, 2005.
31. Cerdà, A.; Robichaud, P. *Fire Effects on Soils and Restoration Strategies. Land Reconstruction and Management Series*; Science Publishers: Enfield, NH, USA, 2009.
32. Robichaud, P.R.; Wagenbrenner, J.W.; Brown, R.E.; Wohlgemuth, P.M.; Beyers, J.L. Evaluating the effectiveness of contour-felled log erosion barriers as a post-fire runoff and erosion mitigation treatment in the western United States. *Int. J. Wildl. Fire* **2008**, *17*, 255–273. [[CrossRef](#)]
33. Fox, D.M.; Laaroussi, Y.; Malkinson, L.D.; Maselli, F.; Andrieu, J.; Bottai, L.; Wittenberg, L. POSTFIRE: A model to map forest fire burn scar and estimate runoff and soil erosion risks. *Remote Sens. Appl. Soc. Environ.* **2016**, *4*, 83–91. [[CrossRef](#)]
34. Batelis, S.-C.; Nalbantis, I. Potential Effects of Forest Fires on Streamflow in the Enipeas River Basin, Thessaly, Greece. *Environ. Process.* **2014**, *1*, 73–85. [[CrossRef](#)]
35. Venkatesh, K.; Preethi, K.; Ramesh, H. Evaluating the effects of forest fire on water balance using fire susceptibility maps. *Ecol. Indic.* **2020**, *110*, 105856. [[CrossRef](#)]
36. Mallinis, G.; Maris, F.; Kalinderis, I.; Koutsias, N. Assessment of Post-fire Soil Erosion Risk in Fire-Affected Watersheds Using Remote Sensing and GIS. *GIScience Remote Sens.* **2009**, *46*, 388–410. [[CrossRef](#)]
37. Varela, M.E.; Benito, E.; Keizer, J.J. Wildfire effects on soil erodibility of woodlands in NW Spain. *Land Degrad. Dev.* **2010**, *21*, 75–82. [[CrossRef](#)]
38. Moody, J.A.; Shakesby, R.A.; Robichaud, P.R.; Cannon, S.H.; Martin, D.A. Current research issues related to post-wildfire runoff and erosion processes. *Earth-Sci. Rev.* **2013**, *122*, 10–37. [[CrossRef](#)]

39. Baloutsos, G.; Oikonomou, A.; Kaoukis, K. *Flood Hazard in Drainage Basins after a Fire. Analysis of the Problem and Direct Measurements for Reducing the Impact*; National Foundation of Agricultural Research, Institute of Mediterranean Forest Ecosystems and Woodland Product Technology: Athens, Greece, 2007.
40. White, W.D.; Wells, S.G. Forest-fire devegetation and drainage basin adjustment in mountainous terrain. In *Adjustment of the Fluvial System*; Rhodes, D.D., Williams, G.P., Eds.; Allen and Unwin: New York, NY, USA, 1982; pp. 199–223.
41. Certini, G. Effects of fire on properties of forest soils: A review. *Oecologia* **2005**, *143*, 1–10. [[CrossRef](#)]
42. Chartres, C.J.; Múcher, H.J. The effects of fire on the surface properties and seed germination in two shallow monoliths from a rangeland soil subjected to simulated raindrop impact and water erosion. *Earth Surf. Process. Landf.* **1989**, *14*, 407–417. [[CrossRef](#)]
43. Jordan, P.; Turner, K.; Nicol, D.; Boyer, D. Developing a risk analysis procedure for post-wildfire mass movement and flooding in British Columbia. In Proceedings of the Specialty Conference on Disaster Mitigation, Calgary, AB, Canada, May 2006. Available online: <http://www.for.gov.bc.ca/hfd/pubs/rsi/fsp/Misc/Misc071.pdf> (accessed on 15 May 2022).
44. Areu-Rangel, O.S.; Bonasia, R.; Di Traglia, F.; Del Soldato, M.; Casagli, N. Flood Susceptibility and Sediment Transport Analysis of Stromboli Island after the 3 July 2019 Paroxysmal Explosion. *Sustainability* **2020**, *12*, 3268. [[CrossRef](#)]
45. Diakakis, M. Effects on flood hazard in Marathon plain from the 2009 wildfire in Attica, Greece. In *Advances in the Research of Aquatic Environment*; Lambrakis, N., Stournaras, G., Katsanou, K., Eds.; Springer: Berlin/Heidelberg, Germany, 2011; Volume 1, pp. 155–162. ISBN 978-3-642-19902-8.
46. Evelpidou, N.; Tzouxanioti, M.; Gavalas, T.; Spyrou, E.; Saitis, G.; Petropoulos, A.; Karkani, A. Assessment of Fire Effects on Surface Runoff Erosion Susceptibility: The Case of the Summer 2021 Forest Fires in Greece. *Land* **2022**, *11*, 21. [[CrossRef](#)]
47. Karkani, A.; Evelpidou, N.; Tzouxanioti, M.; Petropoulos, A.; Santangelo, N.; Maroukian, H.; Spyrou, E.; Lakidi, L.; Piacentini, T. Flash Flood Susceptibility Evaluation in Human-Affected Areas Using Geomorphological Methods—The Case of 9 August 2020, Euboea, Greece. A GIS-Based Approach. *GeoHazards* **2021**, *2*, 366–382. [[CrossRef](#)]
48. van Wagtenonk, J.W.; Root, R.R.; Key, C.H. Comparison of AVIRIS and Landsat ETM+ detection capabilities for burn severity. *Remote Sens. Environ.* **2004**, *92*, 397–408. [[CrossRef](#)]
49. Lekkas, E.; Parcharidis, I.; Arianoutsou, M.; Lozios, S.; Mavroulis, S.; Spyrou, N.-I.; Antoniou, V.; Nastos, P.; Mavrouli, M.; Speis, P.; et al. The July–August 2021 Wildfires in Greece. *News. Environ. Disaster Cris. Manag. Strateg.* **2021**, *25*. Available online: https://edcm.edu.gr/images/docs/newsletters/Newsletter_25_2021_July_August_Wildfires_in_Greece.pdf (accessed on 15 May 2022).
50. EEA Corine Land Cover (CLC). 2018. Available online: <https://land.copernicus.eu/pan-european/corine-land-cover/clc2018> (accessed on 21 November 2021).
51. CORINE Corine Land Cover 2018. Available online: <https://land.copernicus.eu/pan-european/corine-land-cover> (accessed on 15 May 2022).
52. Arend, J.L. Infiltration rates of forest soils in the Missouri Ozarks as affected by woods burning and litter removal. *J. For.* **1941**, *39*, 726–728.
53. Papathanasiou, C.; Makropoulos, C.; Mimikou, M. Hydrological modelling for flood forecasting: Calibrating the post-fire initial conditions. *J. Hydrol.* **2015**, *529*, 1838–1850. [[CrossRef](#)]
54. Stoof, C.R.; Vervoort, R.W.; Iwema, J.; van den Elsen, E.; Ferreira, A.J.D.; Ritsema, C.J. Hydrological response of a small catchment burned by experimental fire. *Hydrol. Earth Syst. Sci.* **2012**, *16*, 267–285. [[CrossRef](#)]
55. Yalcin, G.; Akyurek, Z. *Analyzing Flood Vulnerable Areas with Multicriteria Evaluation*; Middle East Technical University: Ankara, Turkey, 2002.
56. Mousavi, S.M.; Roostaei, S.; Rostamzadeh, H. Estimation of flood land use/land cover mapping by regional modelling of flood hazard at sub-basin level case study: Marand basin. *Geomat. Nat. Hazards Risk* **2019**, *10*, 1155–1175. [[CrossRef](#)]
57. Sönmez, O.; Bizimana, H. Flood hazard risk evaluation using fuzzy logic and weightage-based combination methods in geographic information system. *Sci. Iran.* **2021**, *27*, 517–528. [[CrossRef](#)]
58. Bhat, M.S.; Alam, A.; Ahmad, S.; Farooq, H.; Ahmad, B. Flood hazard assessment of upper Jhelum basin using morphometric parameters. *Environ. Earth Sci.* **2019**, *78*, 54. [[CrossRef](#)]
59. Lóczy, D.; Kis, É.; Schweitzer, F. Local flood hazards assessed from channel morphometry along the Tisza River in Hungary. *Geomorphology* **2009**, *113*, 200–209. [[CrossRef](#)]
60. Farhan, Y.; Anaba, O. Flash Flood Risk Estimation of Wadi Yutum (Southern Jordan) Watershed Using GIS Based Morphometric Analysis and Remote Sensing Techniques. *Open J. Mod. Hydrol.* **2016**, *06*, 79–100. [[CrossRef](#)]
61. Cosandey, C.; Andréassian, V.; Martin, C.; Didon-Lescot, J.F.; Lavabre, J.; Folton, N.; Mathys, N.; Richard, D. The hydrological impact of the mediterranean forest: A review of French research. *J. Hydrol.* **2005**, *301*, 235–249. [[CrossRef](#)]
62. Theochari, A.-P.; Baltas, E. Holistic hydrological approach to the fire event on August 2021 in Evia, Greece. *Euro-Mediterr. J. Environ. Integr.* **2022**, *7*, 287–298. [[CrossRef](#)]

-
63. Diakakis, M.; Nikolopoulos, E.I.; Mavroulis, S.; Vassilakis, E.; Korakaki, E. Observational evidence on the effects of mega-fires on the frequency of hydrogeomorphic hazards. The case of the Peloponnese fires of 2007 in Greece. *Sci. Total Environ.* **2017**, *592*, 262–276. [[CrossRef](#)]
 64. Alonistioti, D.; Papathanasiou, C.; Kasella, A.; Makropoulos, C.; Mimikou, M. Assessing the impact of forest fires on the hydrological response of urban catchments: The case of the eastern Attica region. In Proceedings of the 12th International Conference of Environmental Science and Technology, Rhodes, Greece, 8–10 October 2011; pp. 8–10.

Disclaimer/Publisher’s Note: The statements, opinions and data contained in all publications are solely those of the individual author(s) and contributor(s) and not of MDPI and/or the editor(s). MDPI and/or the editor(s) disclaim responsibility for any injury to people or property resulting from any ideas, methods, instructions or products referred to in the content.